

Singlet-triplet radiative transitions in silicon nanocrystals with shallow donors

© S.A. Fomichev, V.A. Burdov

Lobachevsky State University,
603025 Nizhny Novgorod, Russia
E-mail: serg.foms@mail.ru

Received May 11, 2023

Revised June 26, 2023

Accepted October 30, 2023

Within the framework of the envelope function approximation, the rates of intraband radiative transitions in silicon nanocrystals with donors are calculated. It is shown that for nanocrystals of sufficiently small sizes (about two nanometers in diameter), the singlet level splitting off from the rest of the spectrum in the conduction band, arising due to the short-range potential of the donor ion, can be sufficiently strong (more than eV for a bismuth atom), which makes emission in the visible range possible. The rates of radiative transitions turn out to be on the order of inverse microseconds. At the same time, in the case of intraband transitions, Auger recombination can be completely eliminated and, thereby, the quantum efficiency of the luminescence process is significantly increased.

Keywords: silicon nanocrystal, donor, radiative recombination, intraband transition, recombination rate.

DOI: 10.61011/SC.2023.07.57423.5070C

Optical properties of silicon nanostructures and, in particular, nanocrystals remain the subject of close attention of researchers. It was previously shown that the increase in the rates of interband radiative recombination in them can be achieved by introducing a small donor impurity, such as lithium or phosphor [1–3], into the nanocrystal. However, in the case of interband transitions, the presence of a donor in the nanocrystal manifests itself in two ways. On one hand, the donor ion modifies the electronic wave functions, which may lead to an increase in the probability of emission transitions. On the other hand, the presence of an „extra“ electron in the conduction band coming from the donor actually opens a channel for nonradiative relaxation via the Auger process, which is usually much faster than the radiative interband transition. The inclusion of a fast Auger process leads to efficient photoluminescence quenching.

In this work, an alternative option of using donors in silicon nanocrystals to produce light emission in them is considered. As is well known [4], in bulk silicon the ground (singlet) state for V group donors is strongly detached from the rest of the spectrum in the conduction band, which is due to the short-range donor potential inducing valley-orbit interaction. In nanocrystals, this effect is greatly enhanced by dimensional quantization — the magnitude of the energy gap between the levels of the ground (singlet) and first excited (triplet) states can be tenths of an electron-volt or even more than an electron-volt, depending on the donor introduced into the nanocrystal. At the same time, the fundamental optical slit of a silicon nanocrystal usually has values several times larger.

Singlet-triplet emission transitions occurring inside the conduction zone, i.e., intraband, are not forbidden by the tetrahedral symmetry of the system. It is always possible to choose the energy of the photo-excitation quantum so that it is larger than the singlet energy–triplet splitting,

but significantly smaller than the optical slit width. As a result of absorption of a quantum of light, an electron from the singlet level moves to some higher level in the conduction band, after which it can nonradiatively relax to the triplet level and make a radiative singlet-triplet transition, as shown schematically in Figure 1. In this case, additional electron-hole pairs initiating the Auger process do not arise in the system. As a consequence, the quantum efficiency of photon generation in a nanocrystal can increase significantly. In connection with this, it is of interest to estimate the rates of intraband singlet–triplet transitions in silicon nanocrystals with donors.

We model a silicon nanocrystal in a matrix of a wide-gap dielectric as an infinitely deep spherical potential pit of radius R , in the center of which the donor is located. The

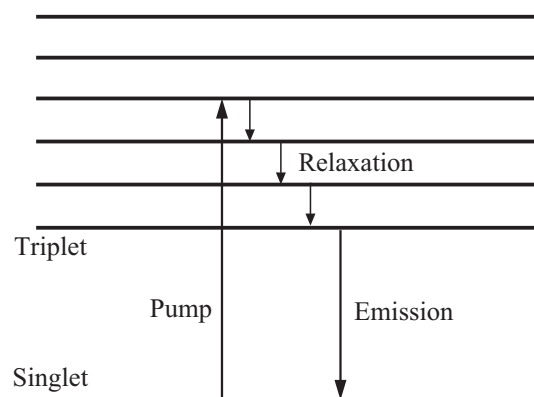


Figure 1. Schematic of levels in the conduction band of a silicon nanocrystal with a donor. The arrows show the processes: excitation of an electron from the singlet level into the zone; nonradiative relaxation to the triplet level; emission transition of the triplet–singlet.

problem of splitting the energy level of the ground state in the conduction band of a nanocrystal, which is sixfold degenerate in the absence of the valley-orbital interaction and the short-range potential of the donor ion, was solved in [5] using the envelope approximation. As in bulk silicon [6], the level splits into a singlet, doublet and triplet, whose wave functions, due to the tetrahedral symmetry of the system, are transformed by three irreducible representations of the tetrahedron group: A_1 , E and T_2 .

The singlet-triplet splitting energy is [5]

$$E_0 = -\frac{W}{2} + \sqrt{\left(\frac{\delta E - W}{2} - H_{pp}\right)^2 + H_{sp}^2} - \sqrt{\left(\frac{\delta E}{2} - H_{pp}\right)^2 + H_{sp}^2}. \quad (1)$$

Here,

$$H_{sp} = \frac{2\hbar p_0}{\sqrt{3}m_i R} \frac{\pi\mu}{\mu^2 - \pi^2}, \quad H_{pp} = \left(\frac{1}{m_t} - \frac{1}{m_l}\right) \frac{\hbar^2 \mu^2}{15R^2},$$

$$\delta E = \frac{\hbar^2(\mu^2 - \pi^2)}{2m_e R^2},$$

where $m_l \approx 0.92m_0$ and $m_t \approx 0.19m_0$ [7] (m_0 — free electron mass), $p_0 = \hbar k_0 \approx 0.152\pi\hbar/a_0$ (a_0 — silicon lattice constant) — the distance in momentum space between one of the X -points and the nearest conduction band minimum [8], and $\mu = 4.4934$ — the first root of the spherical Bessel function $j_1(x)$. The parameter W represents the matrix element of the short-range potential of the donor ion and can be expressed in terms of the shift Δ of the singlet level in bulk silicon relative to the calculated value of the ground state energy level of the hydrogen-like donor, which is 31.3 meV [9], as [5]

$$W = -\frac{\pi^2 a^2 b \Delta}{2R^3}, \quad (2)$$

where $a = 1.02\hbar^2 \varepsilon / (m_e e^2)$, $b = 0.58\hbar^2 \varepsilon / (m_e e^2)$ — variation parameters [6].

The dependence of E_0 on the nanocrystal radius for the three donors V group — P, As, and Bi — is shown in Figure 2. The shift values Δ for these three donors are [4]: 14.2 MeV for phosphorus; 22.4 MeV for arsenic; 40 MeV for bismuth. According to (2) and (1), the highest value of E_0 is achieved when an atom Bi is introduced into the nanocrystal. At the same time, as can be seen from Figure 2, for small nanocrystals with radii ~ 1 nm, the value of the splitting energy reaches values ~ 1.5 eV.

The probability of a singlet-triplet intraband transition occurring per unit time due to photon absorption (transition rate) is determined by the golden rule of quantum mechanics, which, after summing over all possible wave vectors and polarizations of the photon, takes the form

$$\tau^{-1} = \frac{4e^2 \kappa \sqrt{\varepsilon_0} E_0}{3m_0^2 \hbar^2 c^3} |\mathbf{p}_{st}|^2, \quad (3)$$

where \mathbf{p}_{st} — the matrix element of the momentum operator for the singlet-triplet emission transition, ε_0 — the dielectric

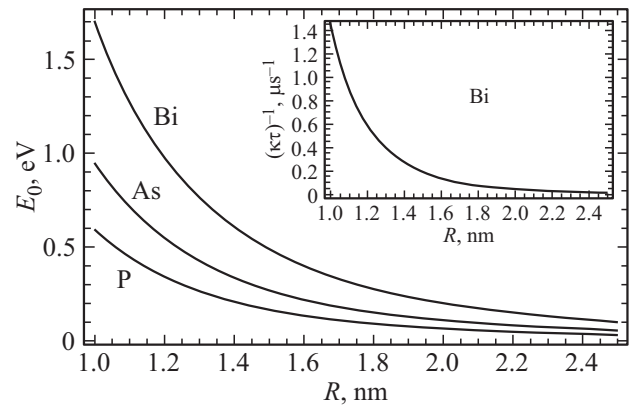


Figure 2. Singlet–triplet splitting energy as a function of nanocrystal radius for three donors — P, As, Bi. On inset — the radiative singlet–triplet transition rate attributed to the parameter κ , as a function of radius for a nanocrystal with a bismuth atom.

permittivity of the matrix surrounding the nanocrystal, and the parameter $\kappa = (3\varepsilon_0/(2\varepsilon_0 + \varepsilon))^2$ accounts for the difference of dielectric permittivities in the nanocrystal and dielectric [10].

For the square of the matrix element of the momentum operator we obtain the expression

$$|\mathbf{p}_{st}|^2 = \sin^2(\lambda_s + \lambda_t) \left(\frac{2\pi\hbar}{3R}\right)^2 \left(\frac{\mu}{\mu^2 - \pi^2}\right)^2, \quad (4)$$

where λ_s and λ_t for the singlet and triplet, respectively, are given by the relations of the form

$$\cos(2\lambda_s) = \frac{\delta E - 2H_{pp} - W}{\sqrt{(\delta E - 2H_{pp} - W)^2 + 4H_{sp}^2}},$$

$$\cos(2\lambda_t) = \frac{\delta E - 2H_{pp}}{\sqrt{(\delta E - 2H_{pp})^2 + 4H_{sp}^2}}$$

and vary in the range $0 \leq \lambda_{s,t} \leq \pi/2$.

The inset in Figure 2 illustrates the dependence of the intraband emission transition rate on the radius of the nanocrystal with the Bi atom. Since the exact value of the dielectric constant of the nanocrystal is unknown, the parameter κ in (3) also cannot be calculated rigorously. For this reason, the plot shows the velocity-to-parameter relationship κ , which is actually equivalent to the velocity at the maximum possible value of $\kappa = 1$. As can be seen from the figure, for nanocrystals with radii of the order of one to one and a half nanometers, the transition rate turns out to be $\sim 10^5 - 10^6 \text{ s}^{-1}$. The values obtained are quite high. If we compare them with the calculated values of the rates of interband emission transitions in nanocrystals based on direct-gap semiconductors (see, for example, the work [11], where the radiative recombination rates for CdSe nanocrystals were calculated, or reviews [12,13]), they will be inferior to the latter only two or three orders of magnitude. It should

be noted that the real parameter determining the smallness of the intraband transition rate in a silicon nanocrystal compared to the interband transition rate in a nanocrystal based on a direct-gap semiconductor is the square of the ratio of the lattice constant to the nanocrystal size: $(a_0/R)^2$. Accordingly, in silicon nanocrystals with diameters smaller than a nanometer, the rates of intraband transitions can be comparable to the rates of interband transitions in nanocrystals based on direct-gap semiconductors. For such small nanocrystals, however, the spherical potential well model and the envelope approximation will no longer be well founded — in this case it is better to use, for example, *ab initio* calculations.

Comparing intraband and direct interband transitions in nanocrystals, we also note that the rates of direct interband transitions depend weakly on the size of the nanocrystal. Their dependence is determined only by the optical slit width, which tends to the band gap width of the bulk material as the radius of the nanocrystal increases. In contrast, the rates of intraband transitions are quite strongly size-dependent. This dependence is determined by the square of the matrix element (4), which is inversely proportional to the square of the radius, and by the transition energy E_0 , which decreases to zero as the nanocrystal size increases. For this reason, as noted above, the process of photon generation will have the greatest efficiency for small nanocrystals, in which it is possible (in the case of the introduction of a bismuth atom into the nanocrystal) to obtain radiation of the visible range.

Finally, let us also make a small remark concerning the case of non-central location of the donor in the nanocrystal. As shown earlier (see work [5]), in this case the doublet and triplet split into two and three levels, respectively. However, this splitting turns out to be negligible (hundredths eV), while the singlet–triplet splitting energy remains approximately the same as for the centrally located donor, up to donor displacements equal to approximately half of the nanocrystal radius. The wave functions of the electrons also do not undergo significant changes, which suggests that the values of the radiative intraband transition rates remain unchanged (at least on the order of magnitude). Thus, the results obtained above for the centrosymmetric case can be applied, at least at a qualitative level, to nanocrystals in which the donor is shifted relative to the center by an amount less than or of the order of half of the radius nanocrystal.

Funding

This study was supported by grant No. 22-79-00281 from the Russian Science Foundation.

Conflict of interest

The authors declare that they have no conflict of interest.

References

- [1] M. Fujii, A. Mimura, S. Hayashi, K. Yamamoto. *Appl. Phys. Lett.*, **75**, 184 (1999).
- [2] E. Klimesova, K. Kusova, J. Vacik, V. Holy, I. Pelant. *J. Appl. Phys.*, **112**, 064322 (2012).
- [3] V.A. Belyakov, A.I. Belov, A.N. Mikhaylov, D.I. Tetelbaum, V.A. Burdov. *J. Phys.: Condens. Matter*, **21**, 045803 (2009).
- [4] R.L. Aggarwal, A.K. Ramdas. *Phys. Rev.*, **140**, A1246 (1965).
- [5] V.A. Belyakov, V.A. Burdov. *Phys. Rev. B*, **76**, 045335 (2007).
- [6] W. Kohn, J.M. Luttinger. *Phys. Rev.*, **98**, 915 (1955).
- [7] J.C. Hensel, H. Hasegawa, M. Nakayama. *Phys. Rev.*, **138**, A225 (1965).
- [8] J.L. Ivey, R.L. Micher. *Phys. Rev. B*, **11**, 822 (1975).
- [9] R.A. Faulkner. *Phys. Rev.*, **184**, 713 (1969).
- [10] A. Thranhardt, C. Ell, G. Khitrova, H.M. Gibbs. *Phys. Rev. B*, **65**, 035327 (2002).
- [11] A.L. Efros. *Phys. Rev. B*, **46**, 7448 (1992).
- [12] V.A. Burdov. M.I. Vasilevskiy. *Appl. Sci.*, **11**, 497 (2021).
- [13] N.V. Derbenyova, A.A. Konakov, V.A. Burdov. *J. Luminesc.*, **233**, 117904 (2021).

Translated by Ego Translating